

# Highly Ordered Macroporous Gold and Platinum Films Formed by Electrochemical Deposition through Templates Assembled from Submicron Diameter Monodisperse Polystyrene Spheres

P. N. Bartlett,<sup>\*,†</sup> J. J. Baumberg,<sup>‡</sup> Peter R. Birkin,<sup>†</sup> M. A. Ghanem,<sup>†</sup> and M. C. Netti<sup>‡</sup>

Department of Chemistry, University of Southampton, Highfield, Southampton, SO17 1BJ, United Kingdom, and Department of Physics & Astronomy, University of Southampton, Highfield, Southampton, SO17 1BJ, United Kingdom

Received November 9, 2001. Revised Manuscript Received February 4, 2002

Here we report a simple and versatile technique for the preparation of novel macroporous three-dimensional gold and platinum films with regular submicron spherical holes arranged in a close-packed structure. Gold and platinum films were prepared by electrochemical reduction of gold or platinum complex ions dissolved in aqueous solution within the interstitial spaces between polystyrene latex spheres (500 or 750 nm in diameter) assembled on gold surfaces. The latex sphere templates were subsequently removed by dissolving in toluene to leave the structured metal films. Scanning electron microscopy of the gold and platinum films shows a well-formed regular three-dimensional, porous structure consisting of spherical voids arranged in a highly ordered face-centered cubic (fcc) structure. The spherical voids have the same diameter as the latex spheres used to form the template. Within the metal film the spherical voids are interconnected through a series of smaller pores. The metallic framework is dense, self-supporting, and free from defects. X-ray studies show the metal to be polycrystalline with a grain size smaller than 100 nm. The optical reflectivity of the macroporous gold and platinum films shows strong diffractive optical properties, which are potentially useful in many existing and emerging applications.

## Introduction

Several chemical preparations of ordered macroporous materials based on colloidal crystal templates (or artificial opals) have been described.<sup>1–19</sup> These methods use

close-packed arrays of monodisperse spheres (typically polystyrene or silica) as templates for the formation of three-dimensionally ordered macroporous structures in a range of materials, such as silica,<sup>1–4</sup> metal oxides,<sup>5–8</sup> metals,<sup>9–12</sup> metal chalcogenides,<sup>13</sup> carbon,<sup>14</sup> polymers,<sup>15–18</sup> and metal alloys.<sup>19</sup> Because the pore diameters of these macrostructures (typically a few hundred nanometers) are similar to the wavelength of visible light, they can be used to create photonic crystals or photonic mirrors, which exhibit interesting optical properties based on Bragg diffraction and the formation of optical photonic band gaps.<sup>6,20</sup>

In general, bulk samples of these materials have been formed by infiltration of the spaces between the template spheres by a concentrated solution of a chemical precursor to the desired material, followed by the conversion of this precursor by some chemical reaction into the desired macroporous material. For example, samples of periodic macroporous metals have now been prepared by several methods including hydrogen reduc-

\* Corresponding author.

<sup>†</sup> Department of Chemistry.

<sup>‡</sup> Department of Physics & Astronomy.

(1) Velev, O. D.; Jede, T. A.; Lobo, R. F.; Lenhoff, A. M. *Nature* **1997**, *389*, 447.

(2) Velev, O. D.; Jede, T. A.; Lobo, R. F.; Lenhoff, A. M. *Chem. Mater.* **1998**, *10*, 3597.

(3) Holland, B. T.; Blanford, C. F.; Do, T.; Stein, A. *Chem. Mater.* **1999**, *11*, 795.

(4) Holland, B. T.; Abrams, L.; Stein, A. *J. Am. Chem. Soc.* **1999**, *121*, 4308.

(5) Holland, B. T.; Blanford, C. F.; Do, T.; Stein, A. *Science* **1998**, *281*, 538.

(6) Wijnhoven, J. E. G. J.; Vos, W. L. *Science* **1998**, *281*, 802.

(7) Yan, H.; Blanford, C. F.; Holland, B. T.; Smyrl, W. H.; Stein, A. *Chem. Mater.* **2000**, *12*, 1134.

(8) Yang, P.; Deng, T.; Zhao, D.; Feng, P.; Pine, D.; Chmelka, B. F.; Whitesides, G. M.; Stucky, G. D. *Science* **1998**, *282*, 2244.

(9) Yan, H.; Blanford, C. F.; Holland, B. T.; Parent, M.; Smyrl, W. H.; Stein, A. *Adv. Mater.* **1999**, *11*, 1003.

(10) Jiang, P.; Cizeron, J.; Bertone, J. F.; Colvin, V. L. *J. Am. Chem. Soc.* **1999**, *121*, 7957.

(11) Velev, O. D.; Tessier, P. M.; Lenhoff, A. M.; Kaler, E. W. *Nature* **1999**, *401*, 548.

(12) Xu, L.; Zhou, W. L.; Frommen, C.; Baughman, R. H.; Zakhidov, A. A.; Malkinski, L.; Wang, J. Q.; Wiley, J. B. *J. Chem. Soc., Chem. Commun.* **2000**, 997.

(13) Vlasov, Y. A.; Yao, N.; Norris, D. J. *Adv. Mater.* **1999**, *11*, 165.

(14) Zakhidov, A. A.; Baughman, R. H.; Iqbal, Z.; Cui, C.; Khayrullin, I.; Dantas, S. O.; Marti, J.; Ralchenko, V. G. *Science* **1998**, *282*, 897.

(15) Park, S. H.; Xia, Y. *Chem. Mater.* **1998**, *10*, 1745.

(16) Park, S. H.; Xia, Y. *Adv. Mater.* **1998**, *10*, 1045.

(17) Johnson, S. A.; Ollivier, P. J.; Mallouk, T. E. *Science* **1999**, *283*, 963.

(18) Jiang, P.; Hawang, K. S.; Mittleman, D. M.; Bertone, J. F.; Colvin, V. L. *J. Am. Chem. Soc.* **1999**, *121*, 11630.

(19) Yan, H.; Blanford, C. F.; Smyrl, W. H.; Stein, A. *J. Chem. Soc., Chem. Commun.* **2000**, 1477.

(20) Thijssen, M. S.; Sprik, R.; Wijnhoven, J. E. G. J.; Megens, M.; Narayanan, T.; Lagendijk, A.; Vos, A. L. *Phys. Rev. Lett.* **1999**, *83*, 2730.

tion of preformed macroporous oxides,<sup>9</sup> electroless deposition,<sup>10,21</sup> deposition of colloidal gold particles into colloidal crystals,<sup>11</sup> and lithography.<sup>22</sup> Although these methods lead to the formation of three-dimensional macroporous metals, they have several disadvantages. Of necessity, these approaches lead to either significant shrinkage of the structure during its formation, incomplete infilling, or significant microporosity of the material around the spherical pores, or both. In addition the sample may be contaminated by residues from the chemical synthesis and may be chemically or mechanically unstable.

In contrast, electrochemical deposition has several significant advantages, particularly for the deposition of thin, supported films of macroporous materials. Electrochemical deposition ensures a high density of the deposited material within the voids of the template and leads to volume templating of the structure as opposed to surface templating of material around the surface of the template spheres. As a result no shrinkage of the material occurs when the template is removed and no need exists for further processing steps or the use of elevated temperatures. Consequently, the resulting metal film is a true cast of the template structure and the size of the spherical voids within the metal is directly determined by the size of template spheres used. The method is also very flexible in the choice of materials that can be used because numerous metals, alloys, oxides, semiconductors, and conducting polymers can be deposited from solution, both aqueous and nonaqueous, under conditions that are compatible with the template. Furthermore, the use of electrochemical deposition allows fine control over the thickness of the resulting macroporous film through control over the charge passed to deposit the film. This is a unique feature of the approach. Electrochemical deposition is ideal for the production of thin supported layers for applications such as photonic mirrors, because the surface of the electrochemically deposited film can be very uniform. Also, because the template spheres are assembled onto the flat surface of the electrode and because electrochemical deposition occurs from the electrode surface out through the overlying template, the first layer of templated material, deposited out to a thickness comparable with the diameter of the template spheres used, has a different structure from subsequent layers. As we show below, the subsequent growth of the film by electrodeposition out through the template leads to a modulation of the surface topography of the film in a regular manner that will depend on the precise choice of deposition bath and deposition conditions.

Despite these advantages, only a few papers describe the electrochemical deposition of supported thin macroporous films.<sup>23–27</sup> Braun and Wiltzius<sup>23</sup> used this ap-

proach to prepare three-dimensional ordered macroporous films of cadmium selenide and cadmium sulfide. Wijnhoven et al.<sup>24</sup> reported the electrochemical deposition of ordered macroporous gold films by electrochemical deposition through templates assembled from monodisperse silica or polystyrene spheres. The macroporous gold films produced using silica spheres (diameter 111 nm) showed uneven nucleation and nonuniform growth with flat flakes of gold (1  $\mu\text{m}$  length) growing between the domain boundaries and over the top of the silica sphere template. In contrast the film produced by using polystyrene latex spheres as template showed a highly random porous microstructure. In their experiments Wijnhoven et al. heated the samples to 450 °C to remove the polystyrene template because they claimed that dissolving the template in organic solvents led to swelling of the polymer which, in turn, damaged the macroporous metal films. Xu et al.<sup>25</sup> used electrochemical deposition to prepare nickel and gold structures by using templates assembled from 300-nm silica spheres assembled by sedimentation during a period of several months. They found that the gold structures collapsed and were not stable, but they were able to make preliminary magnetic measurements for the nickel structure. In a recent publication we described a simple and versatile technique for the preparation of highly ordered three-dimensional macroporous platinum, palladium, and cobalt films with regular submicron spherical holes arranged in a close-packed structure.<sup>26</sup> The metal films were prepared by electrochemical deposition in the interstitial spaces of a template formed by polystyrene latex spheres self-assembled on gold electrodes followed by removal of the polystyrene template by dissolution in toluene. For these films there was no evidence for disruption of the macroporous metal film caused by swelling of the polymer during dissolution. We have also used this approach to prepare macrostructured films of Ni–Fe alloy and investigated the effects of the size of the spherical voids within the alloy on its magnetic properties.<sup>27</sup> This approach can also be used to deposit ordered macroporous films of conducting polymers.<sup>28,29</sup>

In this article we describe the use of electrochemical deposition through an artificial opal template made from polystyrene spheres assembled on a smooth gold electrode surface to produce thin macroporous films of polycrystalline gold and platinum containing highly ordered regular three-dimensional arrays of interconnected spherical submicron voids arranged in a close packed structure. These films are made by the electrochemical reduction of aqueous solutions of gold or platinum complex ions within the interstitial spaces of templates produced from monodisperse polystyrene latex spheres (500 or 750 nm in diameter) assembled on gold electrode surfaces. After the electrochemical deposition of a metal film of the desired thickness, the latex sphere template is removed by soaking the structure in toluene to dissolve the polystyrene and leave the gold or platinum macroporous film. In all cases these

(21) Kulinowski, K. M.; Jian, P.; Vaswani, H.; Colvin, V. L. *Adv. Mater.* **2000**, *12*, 833.

(22) Jensen, T. R.; Schatz, G. C.; Duyne, R. P. V. *J. Phys. Chem. B* **1999**, *103*, 2394.

(23) Braun, P. V.; Wiltzius, P. *Nature* **1999**, *402*, 603.

(24) Wijnhoven, J. E. G. J.; Zevenhuizen, S. J. M.; Hendriks, M. A.; Vanmaekelbergh, D.; Kelly, J. J.; Vos, W. L. *Adv. Mater.* **2000**, *12*, 888.

(25) Xu, L.; Zhou, W. L.; Frommen, C.; Baughman, R. H.; Zakhidov, A. A.; Malkinski, L.; Wang, J. Q.; Wiley, J. B. *J. Chem. Soc., Chem. Commun.* **2000**, 997.

(26) Bartlett, P. N.; Birkin, P. R.; Ghanem, M. A. *J. Chem. Soc., Chem. Commun.* **2000**, 1671.

(27) Bartlett, P. N.; Ghanem, M. A.; de Groot, P.; Zhukov, A., manuscript in preparation.

(28) T. Sumida, T.; Wada, Y.; Kitamura, T.; Yanagida, S. *J. Chem. Soc., Chem. Commun.* **2000**, 1613.

(29) Bartlett, P. N.; Birkin, P. R.; Ghanem, M. A.; Toh, C.-S. *J. Mater. Chem.* **2001**, *11*, 849.

films were mechanically robust and chemically stable. To the best of our knowledge this is the first report of highly ordered stable macroporous gold films. These films were examined by scanning electron microscopy and X-ray diffraction. In addition, we present some of the first results of a study of the optical properties of these novel macroporous films and demonstrate that they exhibit unique optical properties as a consequence of their macroporous structure.

### Experimental Section

**Materials and Substrates.** All solvents and chemicals were of reagent quality and were used without further purification. The monodisperse polystyrene latex spheres, with diameters of 500 and  $750 \pm 20$  nm, were obtained from Alfa Aesar as a 2.5 wt % solution in water. The commercial cyanide-free gold plating solution (Tech. Gold 25, containing  $7.07 \text{ g dm}^{-3}$  gold) was obtained from Technic Inc. (Cranston, R.I.). Hexachloroplatinic acid,  $\text{H}_2\text{PtCl}_6$  (purity 99.99%), propanol, and the toluene were obtained from Aldrich. The gold electrodes used as substrates were prepared by evaporating 10 nm of a chromium adhesion layer, followed by 200 nm of gold, onto 1-mm-thick glass microscope slides. The gold electrodes were cleaned by sonication in propanol for 1 h followed by rinsing with deionized water. All solutions were freshly prepared using reagent-grade water ( $18 \text{ M}\Omega \text{ cm}$ ) from a Whatman RO80 system coupled to a Whatman "Still Plus" system.

**Instrumentation.** Electrochemical deposition was performed in a conventional three-electrode configuration with an EG&G 273. A large area platinum gauze was used as the counter electrode with a homemade saturated calomel reference electrode (SCE) and the template-coated gold substrate as the working electrode. An analytical scanning electron microscope (JEOL 6400) and X-ray diffractometer (Simens Diffraktometer D5000) using  $\text{Cu K}\alpha$  radiation were used to study the morphology and microstructure of the macroporous films. X-ray diffraction measurements were made on films supported on gold on glass substrates. For these experiments thick uniform mesoporous films were used with the mesoporous film facing the X-ray source so that diffraction was dominated by the mesoporous sample rather than the thin, underlying, gold substrate. The optical measurements were performed by using a white-light laser system (Coherent RegA 100 fs regenerative amplifier with continuum generation) coupled with achromatic collimation through a homemade photonic crystal fiber. Angle-dependent reflectivity measurements were recorded using a spectrometer (Jobin-Yvon Triax 550 with liquid nitrogen-cooled CCD) after a home-built sample goniometer combined with optical microscope.

**Assembly of the Colloidal Templates.** The polystyrene sphere templates were assembled by sticking a 1.0-cm-internal-diameter Teflon ring on to the gold substrate using double-sided tape. Approximately  $0.3 \text{ cm}^3$  of an aqueous suspension of the monodisperse polystyrene spheres of 500- or 750-nm diameter diluted with water to 0.5 wt % was spread over the area of the gold electrode surrounded by the Teflon ring ( $0.785 \text{ cm}^2$ ); this corresponds to forming a template layer about 20  $\mu\text{m}$  thick. The sample was then kept in a saturated humidity chamber for 2 to 3 days and then allowed to dry slowly over a period of 3 to 4 days. After all of the water had evaporated the Teflon ring was removed to leave a circular area covered by the template. The template appears opalescent, as expected, with colors from green to red, depending on the angle of observation, clearly visible when the samples were illuminated from above with white light. The templates are robust and adhere well to the gold substrates. There is no evidence for the re-suspension of the latex particles when they are placed in contact with the deposition solutions.

**Synthesis of Highly Ordered Macroporous Gold and Platinum Films.** The electrochemical deposition was conducted at fixed potentials of  $-0.90$  or  $0.10 \text{ V}$  vs SCE for the gold and platinum films, respectively. All gold and platinum

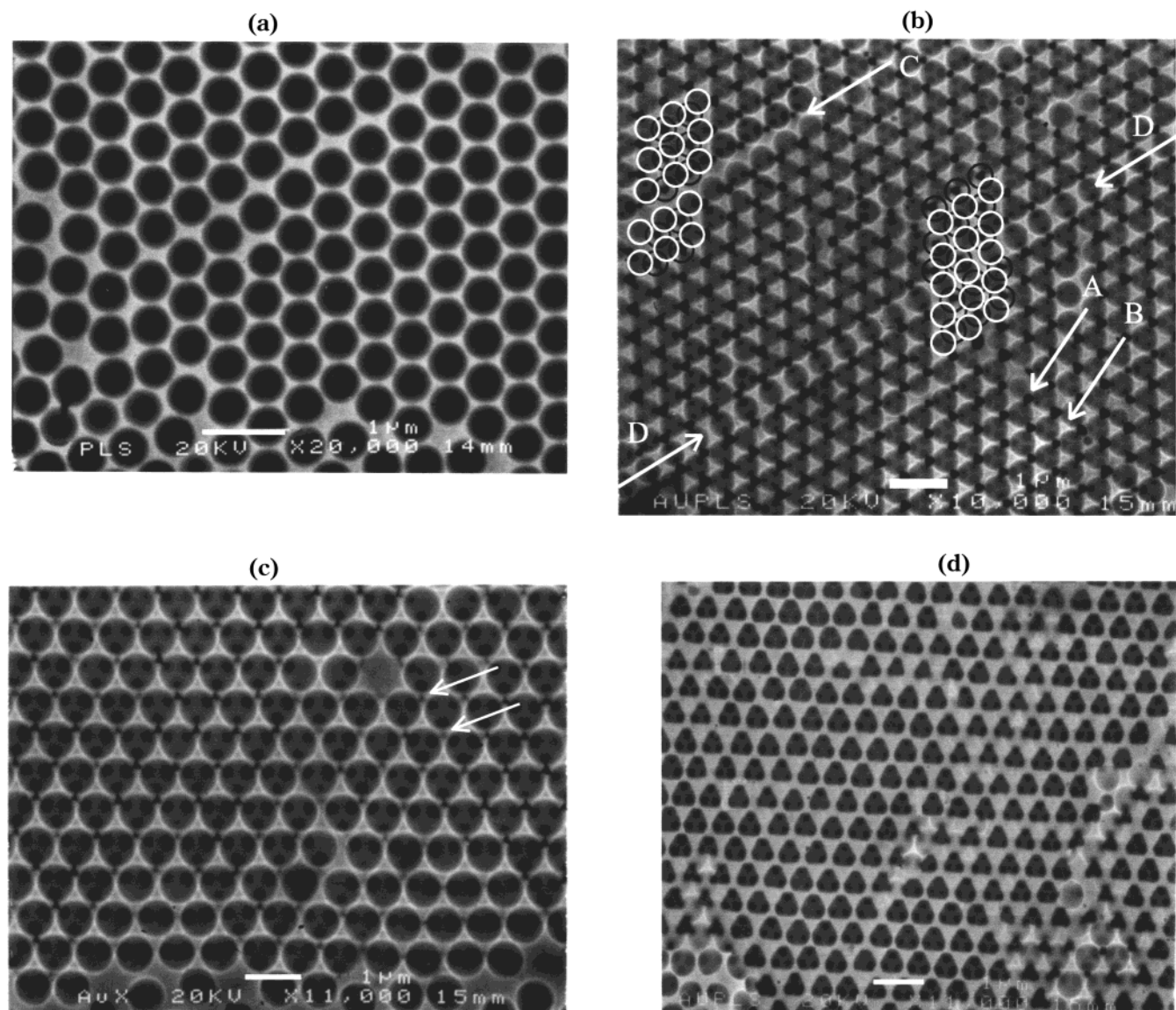
films, unless otherwise stated, were grown with a gradient in thickness ranging from 0.0 to  $1.5 \mu\text{m}$  across the 1 cm diameter sample. This was done in order to allow a systematic study, both by scanning electron microscopy (SEM) and by optical measurements, of the properties of the films as a function of the film thickness. This uniform gradient in film thickness was simply achieved by allowing the plating solution to slowly drain out of the electrochemical cell from a tap in the bottom of the cell while holding the substrate electrode vertical in the cell. After the electrochemical deposition was complete (typically after 25–30 min), the gold and platinum films were soaked in toluene for 24 h to dissolve away the polystyrene template. All experiments were performed at room temperature ( $20\text{--}23 \text{ }^\circ\text{C}$ ).

### Results and Discussion

**SEM Characterization.** All of the electrochemically deposited macroporous films were robust and adhered strongly to the gold substrates. The gold and platinum films are red or dark in appearance, respectively, but show diffractive colors from green to red, depending on the viewing angle, when illuminated from above with white light. Figure 1 shows typical SEM images of different regions of the surface of macroporous gold films grown with a gradient in thickness onto gold substrates covered with templates made up of either  $500 \pm 20$  or  $750 \pm 20$  nm diameter polystyrene spheres. The electrodeposition was performed at a potential of  $-0.90 \text{ V}$  vs SCE with the total charge passed to deposit the film, averaged over the whole electrode area, of  $-1.5 \text{ C cm}^{-2}$  in all cases. The SEM images show that the spherical voids left in the gold films after the removal of the polystyrene spheres are arranged in well-ordered, single-domain, close-packed structures over areas of more than  $150 \mu\text{m}^2$ . Measurements of the center-to-center distances for the pores in Figure 1a and for similar SEM images of other films confirm that the spherical voids within the gold films have the same diameter as the polystyrene spheres used to prepare the template. The separation of the voids is consistent with spheres in the template touching each other.

Figure 1b shows a region of the gold film where the thickness of the film is close to the diameter of the template sphere. At this thickness, because of the geometry of the packing of the spheres in the template, the film has begun to grow around the spheres in the second layer. This is apparent from the small dark triangles and the spherical pores which correspond to the under layer and the upper layer of pores, respectively. To make this clearer we have drawn circles on the image to represent the positions of the original template spheres in the upper layer (light circles) and in the lower layer (dark circles). Note that the dark triangles (marked by arrow A in the figure), representing the pore mouths of the spherical voids within the film, lie directly above the positions of the original template spheres in the bottom layer. Note also that the larger, bright triangular areas, corresponding to the highest points of the metal film (marked by arrow B in the figure), grow up from the underlying substrate through the interstices between the bottom two layers of template spheres. The surface of the film is not smooth and its morphology is controlled by the deposition process as it occurs between the spheres of the template, out from the underlying flat surface of the electrode.





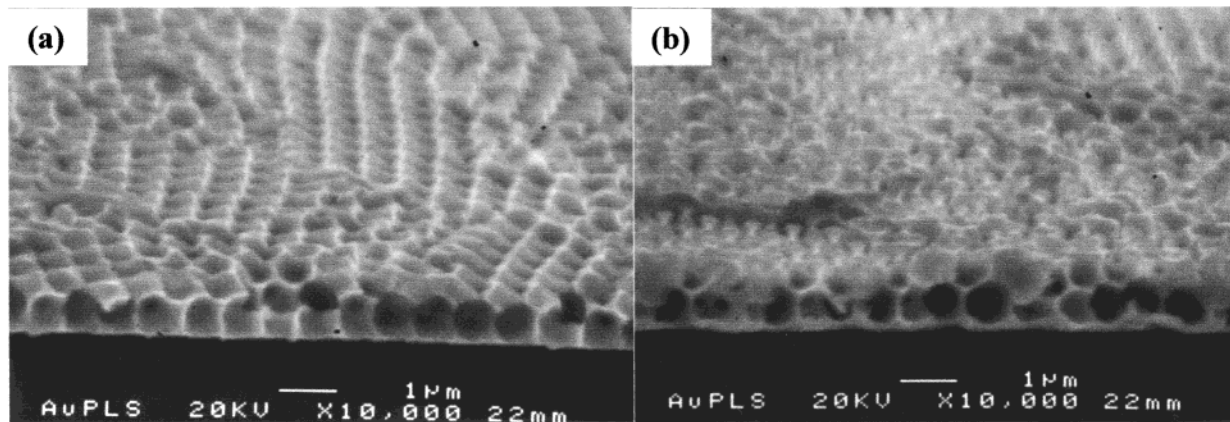
**Figure 1.** SEM images of regions of macroporous gold films grown with a thickness gradient by electrochemical deposition through templates assembled from either 500- or 750-nm-diameter polystyrene spheres. The electrochemical deposition was carried out at  $-0.90$  V vs SCE with a total deposition charge, averaged over the whole electrode area, of  $-1.5$  C  $\text{cm}^{-2}$ . (a) A region where the gold film is about 100 nm thick; pore mouth about 400 nm, and template sphere diameter 500 nm; (b) gold film thickness about 700 nm, template sphere diameter 750 nm; (c) the top-layer pore mouth about 640 nm, gold film thickness about 840 nm, template sphere diameter 750 nm; (d) template sphere diameter 500 nm and gold film thickness equivalent to  $1\frac{3}{4}$  times the template sphere diameter (about 870 nm thick). All scale bars are 1.0  $\mu\text{m}$ .

Figure 1b also shows evidence of packing defects in the original template. See for example the defects marked by arrows C and D. Along the diagonal at C there was a dislocation between the template spheres in the bottom two layers. Along the diagonal at D, in contrast, there was a dislocation in the bottom layer, but this did not carry over into the second layer. (This is a common type of defect in close packing and is known as a Schockley partial.<sup>30</sup>) As a consequence the voids in the top layer along the diagonal D only connect to two voids in the layer below, as shown by the two darker regions within each of these voids as compared with the three darker regions in each of the other voids. In addition we note that above and below the diagonal D the dark triangles representing the mouths of the pores in the bottom layer, and the bright triangles representing the highest points of the metal film, are rotated

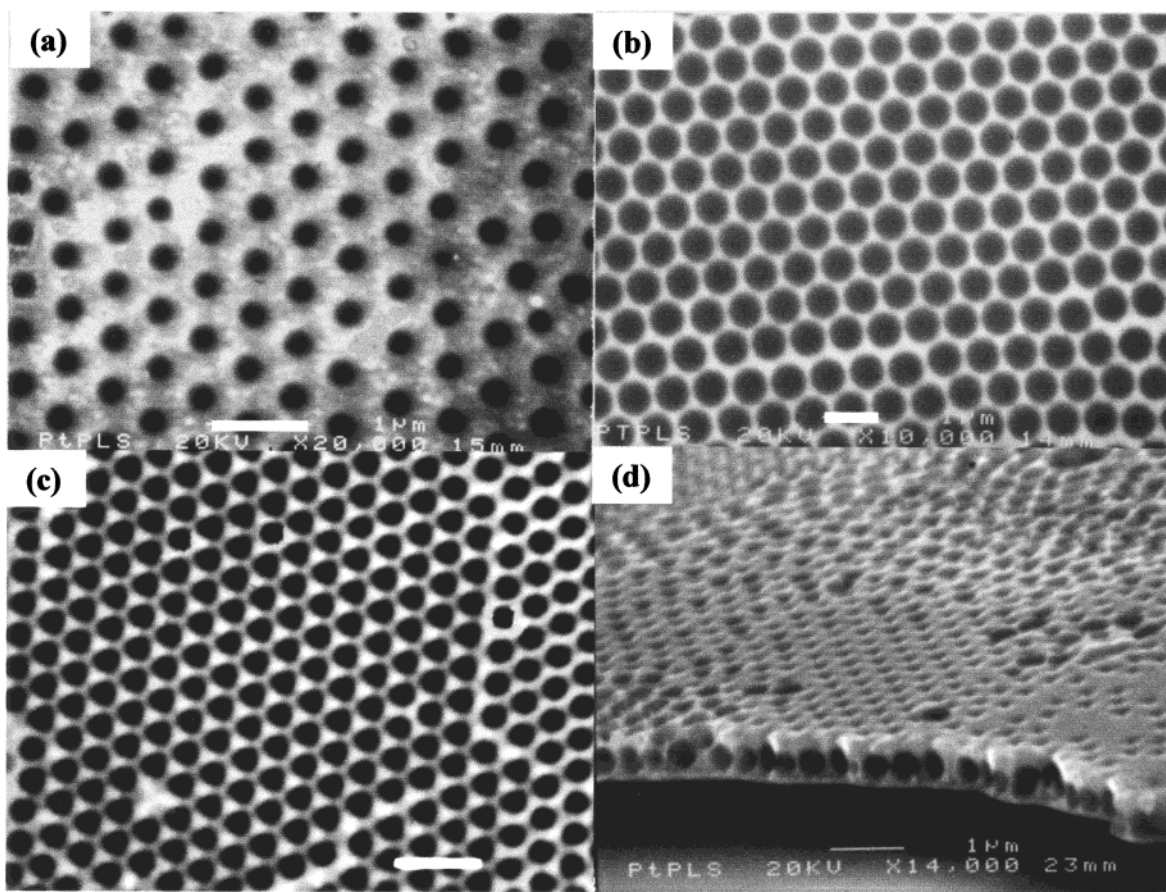
through  $60^\circ$  with respect to each other, again as a consequence of the packing defect.

Figure 1c shows an image for a macroporous gold film prepared through a template of 750-nm-diameter spheres in a region where the film is around 840 nm thick (estimated from the diameter of the mouths of the voids). Within each hemispherical void in the top layer there are again three smaller dark circles (diameter ca. 100 nm). These correspond to the interconnections to the three spherical voids in the layer below that are left around the regions where the original polystyrene spheres in the two layers were in contact. These interconnections between the spherical voids occur because the electrochemical deposition is unable to

(30) Kelly, A.; Groves, G. W. *Crystallography and Crystal Defects*; Longman: Bristol, 1970; p 234.



**Figure 2.** SEM images of macroporous gold films electrochemically deposited under the same conditions as in Figure 1. (a) Image of the edge of a fractured gold film 1 template sphere diameter thick, 750-nm-diameter template sphere; (b) image of the edge of a fractured gold film  $1\frac{1}{2}$  template-sphere diameters thick, 750 nm diameter template sphere. All scale bars are  $1.0\ \mu\text{m}$ .



**Figure 3.** SEM images of regions of macroporous platinum films grown with a thickness gradient by electrochemical deposition through templates assembled from either 500- or 750-nm-diameter polystyrene spheres. The electrochemical deposition was carried from  $50\ \text{mmol}\ \text{dm}^{-3}\ \text{H}_2\text{PtCl}_6$  at 0.10 V vs SCE and the passed charge was  $-1.5\ \text{C}\ \text{cm}^{-2}$  averaged across the whole sample. (a) A platinum film deposited through a template of 500-nm-diameter spheres with a layer thickness of about 17 nm and about 180-nm pore mouth diameter; (b) Pt film which is about 130 nm thick deposited through a template made of 750-nm polystyrene spheres and the pore mouth diameter is  $570 \pm 20\ \text{nm}$ ; (c) Pt film produced using 500-nm latex sphere template with rounded triangular pore mouth diameter about 200 nm and about 370 nm thick; (d) image of a fractured platinum film one of the template-sphere diameter thick, template sphere diameter 500 nm. All scale bars are  $1.0\ \mu\text{m}$ .

completely fill in the narrow regions around the contact points between the separate spheres in the template. Such interconnections have been observed for other porous materials made using colloidal crystal templates.<sup>6,14,10,16,17</sup> Figure 1c also shows evidence for small (typically  $40 \pm 7\ \text{nm}$ ) voids where deposition is incom-

plete at this thickness directly above the center of each spherical void in the lower layer (see, for example, the dark areas marked by the arrows in Figure 1c). Deposition in these regions within the template is blocked by the polystyrene sphere in the lower layer and therefore has to occur by the growth of the metal into this region



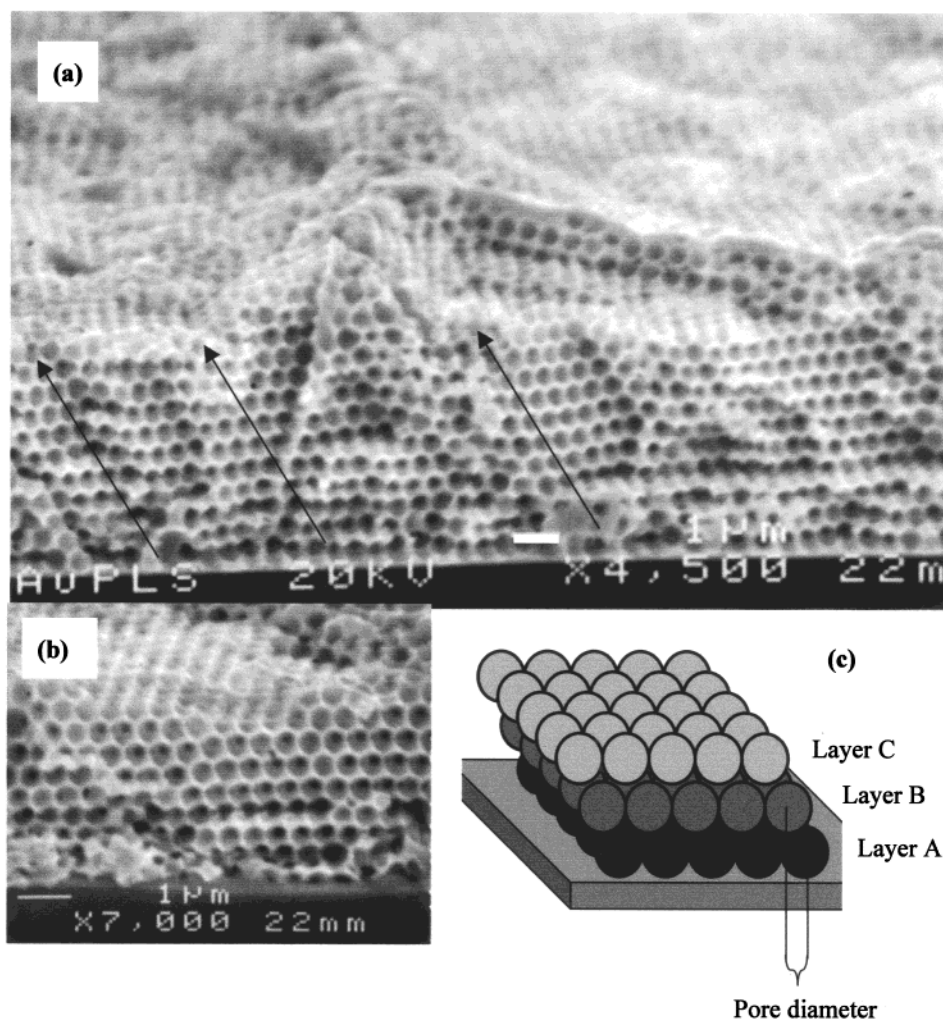


**Figure 4.** (a, b) Images of the fractured edges of a thick macroporous gold film electrochemically deposited through a template formed from 500-nm-diameter polystyrene spheres, deposition potential  $-0.90$  V vs SCE, total charge passed  $2.80$  C  $\text{cm}^{-2}$ . All scale bars are  $1.0$   $\mu\text{m}$ .

from three directions, corresponding to the three columns of metal growing up from the substrate in the interstices between the spheres in the lower level. By scanning across our gradient thickness films we can see that, as the layer gets thicker, these regions become filled in by the metal.

Figure 1d shows an image of a region of the film where it is about  $870$  nm thick. It is noticeable that the pore mouths now have a distinctly rounded triangular shape. Close inspection of the image shows that the rounded triangular pore mouths are all oriented so that the connections to the pores in the layer directly below (shown by the three smaller dark circles within each pore) lie at the vertexes of each rounded triangle.

The advantage of growing films with a gradient of thickness is that by scanning across the film we can follow the evolution of the surface topography of the film as the thickness increases. When we do this we find that the triangular pore mouths seen in Figure 1d are a regular feature of the films when the thickness is close to  $(n + 3/4)$  sphere diameters, where  $n$  is  $0, 1, 2, \dots$  etc.<sup>26</sup> This rounded triangular shape of the pore mouths is a consequence of the way in which, as the electrochemical deposition proceeds out from the planar substrate, it is hindered by the polystyrene spheres so that the surface

of the electrochemically deposited film is not planar. The presence of the template spheres has two effects: the spheres both block the growth of metal out from the substrate and hinder the supply of metal ions from the solution by diffusion to the surface of the growing metal film. It is as a result of the blocking effect that, when the layer is around  $(n + 1/2)$  sphere diameters thick, we find the small voids marked by the arrows in Figure 1c. By the time the layer is up to  $(n + 3/4)$  sphere diameters thick these voids have filled in, but in these regions the film is still not as thick as it is directly above the metal columns growing up through the interstices between the spheres in the lower level. Consequently, around the mouth of the pore in the top layer the height of the metal above the substrate varies in such a way that, when viewed from above, the pore mouth appears triangular, as in Figure 1d, despite the fact that the pore itself is still spherical.

SEM studies on the thickness gradient samples show that these features are repeated cyclically, because the film thickness increases with the appearance of the film surface changing regularly as the film increases in multiples of the template sphere diameter. Thus, the surface topographies are not those that would be expected if the surface of the film were planar and parallel to the substrate surface. Rather, the precise

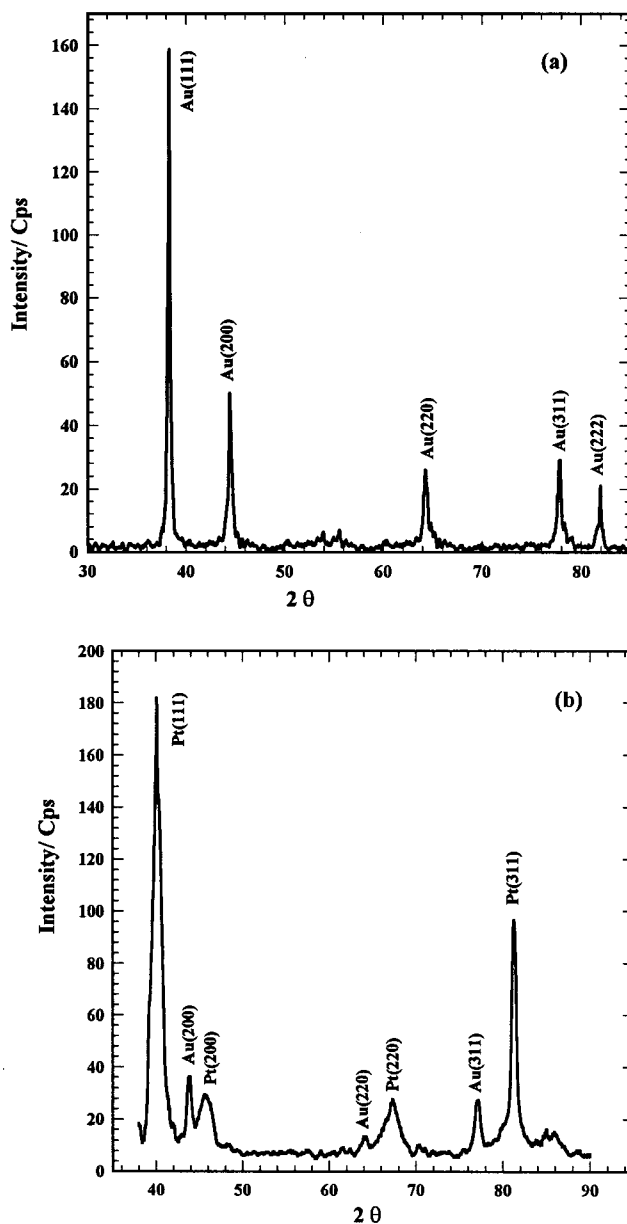
surface topography for films of this type is determined by the interplay of the electrochemical deposition conditions and the structure of the template.

Figure 2a and b shows SEM images of cross sections of gold films prepared by using 750-nm polystyrene sphere templates. In this case the samples were prepared by fracturing the glass slide and supported film after deposition to show a fractured edge. These micrographs again demonstrate the formation of a three-dimensional macroporous Au film, in this case with thicknesses of about 1 and 1.5 times the diameter of the polystyrene spheres used in the template, respectively. These SEM images, and others like them for films of different thicknesses, also directly confirm that the surfaces of the films are not flat, but rather that they have a complex submicron topography.

Figure 3 shows SEM micrographs of the top surface of macroporous Pt films electrochemically deposited from an aqueous 50 mmol dm<sup>-3</sup> solution of hexachloroplatinic acid (H<sub>2</sub>PtCl<sub>6</sub>) at 0.10 V vs SCE. For these films the thicknesses varied linearly from 0.0 to 1.0 μm throughout the 1-cm-diameter samples. The SEM image in Figure 3a corresponds to the surface of a platinum film electrochemically deposited through a template of 500-nm-diameter spheres with a layer thickness of about 17 nm. Where the film is less than half a sphere diameter in thickness, the voids are segments of spheres with circular pore mouths 180 ± 10 nm in diameter and with centers 500 ± 20 nm apart as expected. As the film gets thicker the mouths of the pores get larger and become closer together. Figure 3b shows a micrograph of the surface of a film that was deposited through a template made of 750-nm polystyrene spheres in a region where it is about 130 nm thick. Here the mouths of the pores are 570 ± 20 nm in diameter and the centers of the pores are 750 ± 25 nm apart, as expected for a close-packed array of hemispherical pores formed with a 750-nm template. However, as for the mesoporous gold films discussed above, as the platinum film is grown thicker, the circular shape of the pore mouths changes to rounded hexagonal and triangular shapes depending on the precise thickness of the film in multiples of the template sphere diameter (see Figure 3c and d).

As shown above the spherical voids within the gold or platinum films are packed in ordered hexagonal layers. In principle, these layers can be stacked together in a regular ABAB... sequence corresponding to a hexagonal close-packed structure (hcp), in a regular ABCABC... sequence corresponding to a face-centered cubic structure (fcc), or in a random ABACBAC... sequence corresponding to a random close-packed structure. These different possible close-packed structures have identical packing densities and are indistinguishable from the top surface SEM images of the pores, because at best these images show only the arrangement of the top layer of pores and the layer immediately below that. In the images shown, these top layers correspond to either the (111) plane of the fcc system or the (001) plane of the hcp system.

Although calculations show that for hard sphere packing the fcc structure is the more stable the difference in free energy between the fcc structure and the



**Figure 5.** (a) Powder X-ray diffraction pattern for the macroporous gold film shown in Figure 4 (the film was 5.8 μm thick); (b) typical X-ray powder diffraction pattern for a macroporous platinum film electrochemically deposited through a template assembled from 750-nm polystyrene spheres, charge passed in deposition 3.0 C cm<sup>-2</sup>.

hcp structure is very small (about 0.005 RT per mol).<sup>31</sup> Earlier work by Vos et al.<sup>32</sup> and others<sup>33–35</sup> showed that artificial opals assembled from silica spheres or polystyrene spheres have a fcc structure. However, these templates were assembled by sedimentation over several weeks and not by the method used in the present work, so one should not assume that our templates are necessarily fcc in structure.

- (31) Woodcock, L. V. *Nature* **1997**, *385*, 141.  
 (32) Vos, W. L.; Megens, M.; van Kats, C. M.; Bösecke, P. *Langmuir* **1997**, *13*, 6004.  
 (33) Cheng, B.; Ni, P.; Jin, C.; Li, Z.; Zhang, D.; Dong, P.; Guo, X. *Opt. Commun.* **1999**, *170*, 41.  
 (34) Xia, Y.; Gates, B.; Park, S. H. *J. Lightwave Technol.* **1999**, *17*, 1956.  
 (35) Jiang, P.; Bertone, J. F.; Hwang, K. S.; Colvin, V. L. *Chem. Mater.* **1999**, *11*, 2132.

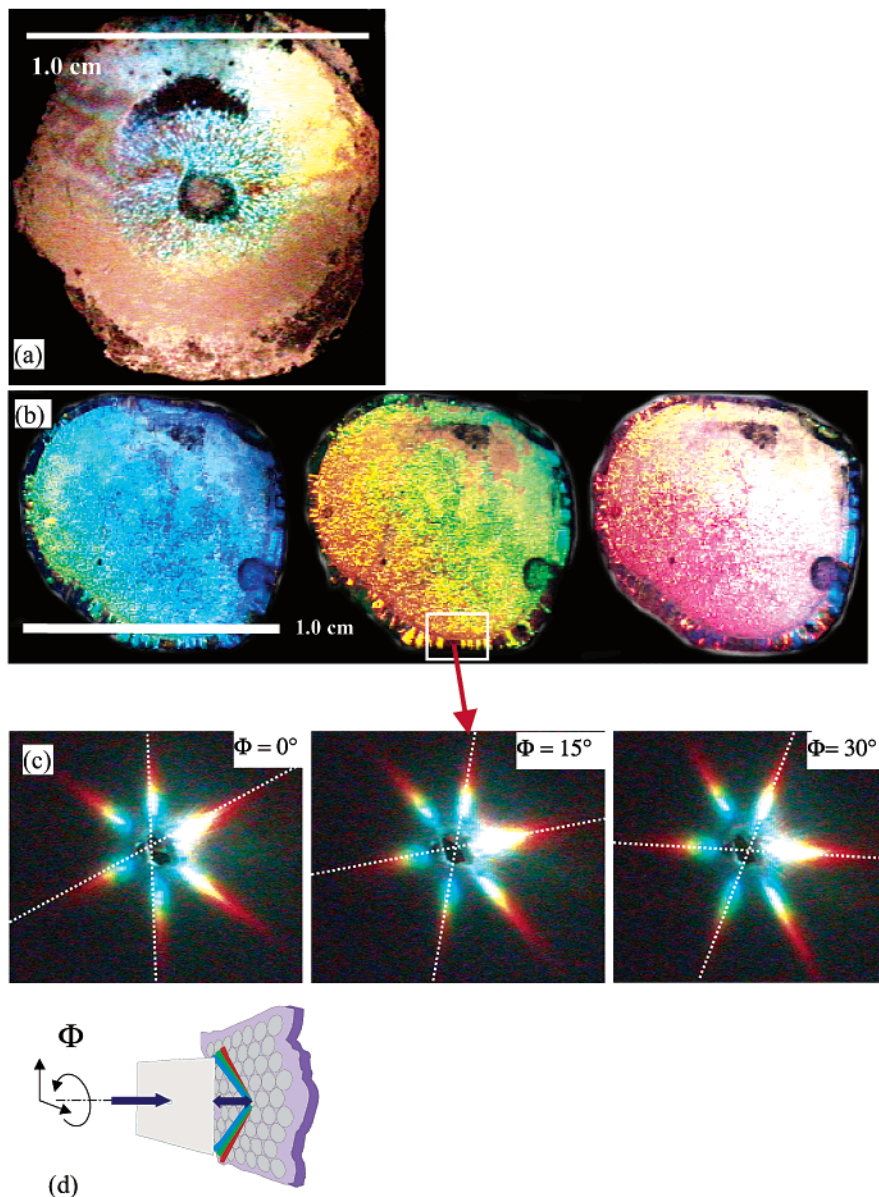


**Figure 6.** Optical appearance of a macroporous Au and Pt film having 750-nm-diameter pores. (a) Image of the Au film when directionally illuminated with white light over a broad area. (b) Image of the Pt film when similarly illuminated with white light. (c) Local diffraction pattern of Pt film obtained by a high-brightness, white-light laser focused onto a small spot on the same sample at normal incidence. The images have different azimuthal orientations,  $\Phi$ , of 0, 15, and 30°. (d) Diagram of the diffraction experiments in c.

To investigate this question we deposited gold macroporous films many multiples of the spherical template diameter in thickness and then fractured these to examine them in cross section. Figure 4a and b shows the cross-sectional SEM images of a macroporous gold film electrochemically deposited through a template of 500-nm polystyrene spheres with a deposition potential of  $-0.90$  V vs SCE and passing a total charge of  $-2.80$  C  $\text{cm}^{-2}$ . From the images we can see that the gold film is about 14 layers of spherical pores in thickness (corresponding to  $5.8 \pm 1.0$   $\mu\text{m}$ ). From the image we can see that the layers of spherical pores are stacked together in the fcc structure ordered (ABCABC ... sequence) with the (111) plane parallel to the substrate and each pore layer shifted from other layers by a distance equal to the pore radius (see the model in Figure 4c). In addition, the higher magnification cross-section SEM image in Figure 4b shows that each larger

pore contains other smaller pores which correspond to the connection to the other neighboring pores in the same layer. The average void-volume fraction of the macroporous gold film is about  $60 \pm 7.15\%$  as calculated from the amount of charge passed in the deposition and the measured film thickness. This is in reasonably good agreement with the value expected (74%) for close packing, the difference between the two values being accounted for by the presence of domain boundaries within our sample.

**X-ray Analysis.** The crystallinity and the crystal structure of the gold and platinum within the walls of the macroporous structure was studied by powder X-ray diffraction. Figure 5a and b shows typical X-ray diffraction patterns obtained from the 5.8- $\mu\text{m}$ -thick macroporous gold film shown in Figure 4a and from a macroporous platinum film electrochemically deposited through a template formed from 500-nm-diameter spheres using



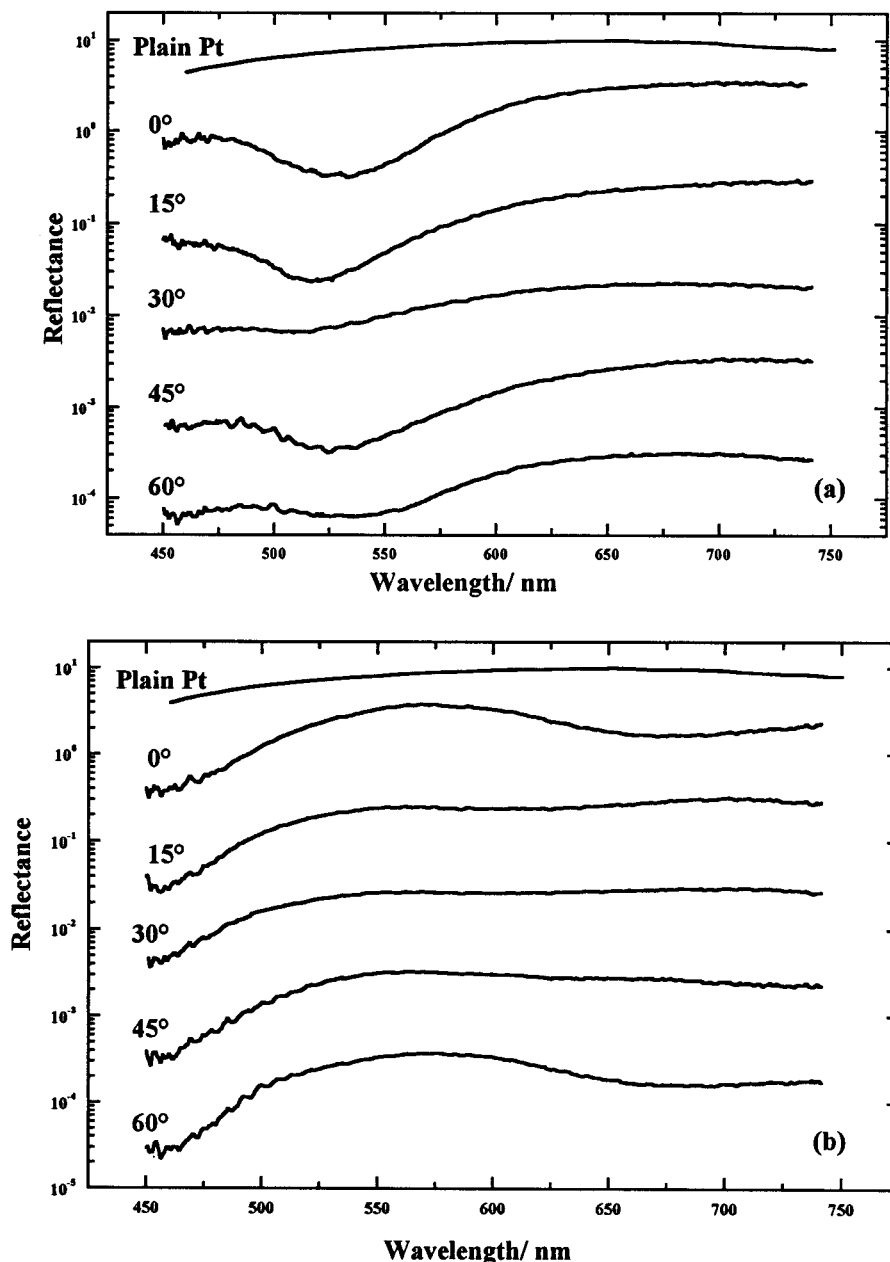


**Figure 7.** Local reflectance spectra on the Pt sample as a function of the azimuthal angle ( $\Phi$ ) for (a) p-polarization and (b) s-polarization. The incidence angle was fixed at  $45^\circ$ . Simultaneously recorded spectra for an unpatterned film are also shown.

a total charge of  $3.0 \text{ C cm}^{-2}$ . The powder X-ray diffraction patterns clearly show the characteristic reflections expected for highly polycrystalline metallic gold and platinum with face-centered cubic (fcc) structures and a preferred (111) orientation.<sup>36</sup> With the Scherrer equation,<sup>37</sup> from the width of the peaks at half-maximum the calculated grain sizes for the gold and platinum are 68 and 8.2 nm, respectively. These grain size dimensions are significantly less than the diameters of the template spheres.

#### Optical Properties of Macroporous Metal Films.

Because the highly ordered structure of the spherical voids within the gold and platinum films and because the pore diameters correspond to the wavelength of visible light, these metal films exhibit optical diffraction

phenomena that lead to striking optical properties. Figure 6a shows a photograph of part of the same macroporous Au film as shown in Figure 1, when a wide area is illuminated with white light from a halogen lamp. From the photograph we can see the color change with increasing thickness of the macroporous Au film, which has a small polycrystalline grain size of  $\sim 10 \mu\text{m}$  in this region. As shown in Figure 6a the packing of the spheres is most uniform in the central region of the sample and is less uniform around the periphery. More details about the optical properties of this Au film will be reported elsewhere.<sup>38,39</sup> Figure 6b shows a corresponding image of a mesoporous platinum film when illuminated with a white light. This reveals areas of the film with small ( $< 10 \mu\text{m}$ ) and large ( $> 100 \mu\text{m}$ ) grain sizes, each of which is differently oriented, resulting in

(36) JCPDS – International Centre for Diffraction Data PCPDF win V 20.1 card no (01–1172) 1998.

(37) Hammond, C. *The Basics of Crystallography and Diffraction*; Oxford University Press: Oxford, 1997.

diffraction of different colors into the imaging camera. Moving the light source results in rapid variations in the color of each crystallite, the phenomenon of opalescence. The diffraction pattern of a single grain from this Pt film is shown in Figure 6c, taken by using a white-light laser<sup>40</sup> focused down onto a 5- $\mu\text{m}$ -diameter spot on the sample using a long-working distance  $\times 16$  microscope objective. The image is recorded for normal incident light passing through a hole in a translucent image plate beyond which it hits the sample as sketched in Figure 6d. The 6-fold diffracted orders are then visible in reflection on the screen, as expected from a two-dimensional diffraction grating. Higher order diffracted orders are also seen if the angle of incidence is increased. The diffracted colors clearly show the expected increase in diffraction angle for longer wavelengths. When the sample is rotated around the focal spot, the orientation of the diffraction pattern similarly rotates. Thus we confirm the films act as diffraction gratings in which the periodicity is not just in a single direction, but along three equivalent directions oriented at 120°. Such two-dimensional diffraction elements can thus be fabricated using self-assembly and electrochemical templating. The blaze of such a grating can be tuned using the control of the surface morphology available by varying the layer thickness, and such data will be presented elsewhere. The control possible through sequential growth of metals and dielectrics in the vertical direction opens up new possibilities for three-dimensional optical interconnection elements.

Measurements of the direct reflectivity spectra of the Pt films in the visible wavelength range are shown in Figure 7. The incident angle is now 45° and so both electric field polarization orientations (*s* and *p*) are shown. The spectra show evidence for weak resonances of reduced reflectivity as compared with an unpatterned Pt film deposited under the same conditions, with an azimuthal periodicity which matches that of the triangular surface lattice. In contrast Au films show dramatic sharp resonances caused by surface plasmon–polariton interactions with the patterned film.<sup>38,39</sup> Plasmons are found only at much higher energies in Pt, and are strongly broadened by damping from coupling to the bulk electrons. The reflectivity dips here are attributed to the different spectral efficiency of diffracting light out of the reflected beam due to the precise shape of the surface structures. Other possibilities include the trapping and scattering of light in the spherical voids, or the interconversion of different polarizations due to the

nonplanar surface morphology. Further work is in progress to assess these possibilities.

## Conclusions

By using templates prepared by assembling close-packed arrays on monodisperse polystyrene spheres, it is possible to electrochemically deposit highly ordered three-dimensional macroporous thin films of gold and platinum in which the spherical voids are arranged in a face-centered close (fcc) structure embedded in the polycrystalline gold or platinum matrix with a void volume fraction of about 60%. The resulting macroporous films of gold and platinum are robust and physically stable when the template is removed and are easily handled in the laboratory. The diameter of the spherical voids is determined by the diameter of the polystyrene latex spheres used to form the template. The spherical voids within the metal films are not isolated, but rather are interconnected by a network of smaller pores. SEM images show that the mouths of the spherical pore are circular in shape if the film thickness is less than the template sphere radius. However, if the film thickness exceeds one template sphere radius then the pore mouths adopt a hexagonal or rounded triangular shape which depends on the precise thickness of the film. The surface topography of these films is determined by the blocking effect of template spheres on the growing metal film.

Powder X-ray analysis shows that the gold and platinum metal in the walls of the macrostructure has the expected fcc structure and is highly polycrystalline with grain sizes significantly smaller than the diameters of the template spheres. We conclude that the electrochemical deposition of metals through assembled templates of monodisperse polystyrene spheres is a simple, quick, and effective method to produce mesoporous films of controlled thickness and pore size that are robust and free from filling defects or problems caused by shrinkage during processing. It is clear that this method can be readily extended to make macroporous films from the wide range of different metals and alloys that can be deposited electrochemically from aqueous solutions.

The preliminary optical properties of the produced macroporous Au and Pt films showed that they function as effective two-dimensional diffractive elements. Controllable variations in the surface morphology can be used to vary the scattering properties of these structures, offering the prospect of low-cost optical functionalities, and new optical effects.

**Acknowledgment.** M.A.G. thanks the embassy of the Arab Republic of Egypt, London, W1Y 8BR, for financial support and Mr. A. Clarke for help with SEM. This work is partly supported by HEFCE JR98SOBA.

CM011272J

(38) Netti, M. C.; Coyle, S.; Baumberg, J. J.; Ghanem, M. A.; Birkin, P. R.; Bartlett, P. N.; Whitaker, D. M. *Adv. Mater.* **2001**, *13*, 1368.

(39) Coyle, S.; Netti, M. C.; Baumberg, J. J.; Ghanem, M. A.; Birkin, P. R.; Bartlett, P. N.; Whitaker, D. M. *Phys. Rev. Lett.* **2001**, *87*, 176801.

(40) Netti, M. C.; Charlton, M. D. B.; Parker, G. J.; Baumberg, J. *J. Appl. Phys. Lett.* **2000**, *76*, 991.